Radiation Dosimetry for ^{177}Lu-PSMA I&T in Metastatic Castration-Resistant Prostate Cancer: Absorbed Dose in Normal Organs and Tumor Lesions

Shozo Okamoto*[1,2], Anne Thieme*[1], Jakob Allmann[1], Calogero D'Alessandria[1], Tobias Maurer[3], Margitta Retz[3], Robert Tauber[3], Matthias M. Heck[3], Hans-Juergen Wester[4], Nagara Tamaki[2], Wolfgang P. Fendler[5], Ken Herrmann[5], Christian H. Pfob[1], Klemens Scheidhauer[1], Markus Schwaiger[1], Sibylle Ziegler†[1], and Matthias Eiber†[1,5]

[1]*Department of Nuclear Medicine, Klinikum Rechts der Isar, Technical University of Munich, Munich, Germany;* [2]*Department of Nuclear Medicine, Hokkaido University Graduate School of Medicine, Sapporo, Japan;* [3]*Department of Urology, Klinikum Rechts der Isar, Technical University of Munich, Munich, Germany;* [4]*Chair of Pharmaceutical Radiochemistry, Technical University of Munich, Munich, Germany; and* [5]*Department of Molecular and Medical Pharmacology, David Geffen School of Medicine at UCLA, Los Angeles, California*

Prostate-specific membrane antigen (PSMA)–targeted radioligand therapy is increasingly used in metastatic castration-resistant prostate cancer. We aimed to estimate the absorbed doses for normal organs and tumor lesions using ^{177}Lu-PSMA I&T (I&T is imaging and therapy) in patients undergoing up to 4 cycles of radioligand therapy. Results were compared with pretherapeutic Glu-NH-CO-NH-Lys-(Ahx)-[^{68}Ga(HBEDCC)] (^{68}Ga-PSMA-HBED-CC) PET. **Methods:** A total of 34 cycles in 18 patients were analyzed retrospectively. In 15 patients the first, in 9 the second, in 5 the third, and in 5 the fourth cycle was analyzed, respectively. Whole-body scintigraphy was performed at least between 30–120 min, 24 h, and 6–8 d after administration. Regions of interest covering the whole body, organs, and up to 4 tumor lesions were drawn. Organ and tumor masses were derived from pretherapeutic ^{68}Ga-PSMA-HBED-CC PET/CT. Absorbed doses for individual cycles were calculated using OLINDA/EXM. SUVs from pretherapeutic PET were compared with absorbed doses and with change of SUV. **Results:** The mean whole-body effective dose for all cycles was 0.06 ± 0.03 Sv/GBq. The mean absorbed organ doses were 0.72 ± 0.21 Gy/GBq for the kidneys; 0.12 ± 0.06 Gy/GBq for the liver; and 0.55 ± 0.14 Gy/GBq for the parotid, 0.64 ± 0.40 Gy/GBq for the submandibular, and 3.8 ± 1.4 Gy/GBq for the lacrimal glands. Absorbed organ doses were relatively constant among the 4 different cycles. Tumor lesions received a mean absorbed dose per cycle of 3.2 ± 2.6 Gy/GBq (range, 0.22–12 Gy/GBq). Doses to tumor lesions gradually decreased, with 3.5 ± 2.9 Gy/GBq for the first, 3.3 ± 2.5 Gy/GBq for the second, 2.7 ± 2.3 Gy/GBq for the third, and 2.4 ± 2.2 Gy/GBq for the fourth cycle. SUVs of pretherapeutic PET moderately correlated with absorbed dose ($r = 0.44$, $P < 0.001$ for SUV_{max}; $r = 0.43$, $P < 0.001$ for SUV_{mean}) and moderately correlated with the change of SUV ($r = 0.478$, $P < 0.001$ for SUV_{max}, and $r = 0.50$, $P < 0.001$ for SUV_{mean}). **Conclusion:** Organ- and tumor-absorbed doses for ^{177}Lu-PSMA I&T are comparable to recent reports and complement these with information on an excellent correlation between the 4 therapy cycles. With the kidneys representing the critical organ, a cumulative activity of 40 GBq of ^{177}Lu-PSMA I&T appears to be safe and justifiable. The correlation between pretherapeutic SUV and absorbed tumor dose emphasizes the need for PSMA-ligand PET imaging for patient selection.

Key Words: PSMA I&T; prostate cancer; dosimetry; radioligand therapy; response

J Nucl Med 2017; 58:445–450
DOI: 10.2967/jnumed.116.178483

Prostate cancer (PC) is the second most common cancer in men worldwide (*1*). About 30% of men experience biochemical recurrence often followed by progression to metastatic castration-resistant PC (mCRPC). Despite several treatment options for these patients, more than 250,000 men are still dying from PC worldwide each year (*1*). Most recently, prostate-specific membrane antigen (PSMA) is gaining significant interest as a target for imaging as well as radionuclide therapy (*2,3*). Its expression correlates with the malignancy of the disease, being further increased in mCRPC (*4*). A variety of PSMA ligands for radioligand therapy (RLT) have been developed in recent years (*5*). Several studies using ^{131}I- or ^{177}Lu-labeled PSMA ligands for RLT reported reductions in tumor volume and serum prostate-specific antigen (PSA) levels (*3,6–10*). For the assessment of a new radiopharmaceutical, dosimetry is essential to aim for the optimal therapeutic response with limited side effects. Beside the high and specific uptake of PSMA ligands in PC tissue, different normal organs (e.g., kidney, salivary glands, proximal intestine) exhibit tracer accumulation. Recently published studies using the theranostic DOTA-conjugated PSMA ligand ^{177}Lu-PSMA-DKFZ-617 reported results for both posttherapeutic dosimetry (*9,11,12*) and pretherapeutic dosimetry (*13*).

DOTAGA-(I-y)fk(Sub-KuE), termed PSMA I&T for imaging and therapy, is another PSMA ligand (*6*). It also allows the use of ^{68}Ga- and ^{177}Lu-labeled compounds as theranostic twins. Our initial experiences in antitumor effect and side effects in heavily pretreated patients using this agent have been published recently (*10*). Similar results on clinical efficacy were reported by Baum et al. with additional data on dosimetry (*7*). In peptide receptor radionuclide therapy for neuroendocrine tumors, high tumor uptake in pretherapeutic PET and high tumor-absorbed dose are regarded to be predictive of the therapeutic success (*14*). The SUV may serve as indicator for

Received May 18, 2016; revision accepted Aug. 30, 2016.
For correspondence or reprints contact: Matthias Eiber, Department of Nuclear Medicine, Klinikum Rechts der Isar, Technical University of Munich, Ismaniger Strasse 22, Munich, Germany 81675.
E-mail: matthias.eiber@tum.de
*Contributed equally to this work.
†Contributed equally to this work.
Published online Sep. 22, 2016.
COPYRIGHT © 2017 by the Society of Nuclear Medicine and Molecular Imaging.

later-achieved absorbed dose (*15–17*). Presumably, also in mCRPC the decision for or against RLT may be influenced and eventually potentially based on pretherapeutic PET.

Thus, the purpose of this study was to estimate the absorbed doses for ^{177}Lu-PSMA I&T in normal organs and in tumor lesions in a considerable number of patients with mCRPC undergoing up to 4 cycles with a reference activity of 7.4 GBq. In addition, we aimed to investigate the relationship of pretherapeutic SUV of Glu-NH-CO-NH-Lys-(Ahx)-[^{68}Ga(HBEDCC)] (^{68}Ga-PSMA-HBED-CC) PET and subsequently achieved tumor-absorbed dose and tumor response by PET.

MATERIALS AND METHODS

Patients and ^{68}Ga-PSMA-HEBD-CC PET/CT

Between January 2015 and March 2016, 18 patients (Table 1) with mCRPC and PSMA-avid lesions on pretherapeutic PET underwent 34 cycles of ^{177}Lu-PSMA I&T ($n = 15$ for first, $n = 9$ for second, $n = 5$ for third, $n = 5$ for fourth cycle) using a reference activity of 7.4 GBq combined with a dedicated protocol for posttherapy dosimetry. The institutional review board of the Technische Universität München approved this study, and all subjects signed a written informed consent form.

^{177}Lu-PSMA I&T RLT and Posttherapy Scintigraphy

The mean applied activity for all cycles was 7.3 ± 0.30 GBq (range, 6.47–7.83 GBq), 7.3 ± 0.32 GBq (range, 6.47–7.78 GBq) for the first cycle, 7.3 ± 0.34 GBq (range, 6.47–7.73 GBq) for the second cycle, 7.5 ± 0.22 GBq (range, 7.30–7.83 GBq) for the third cycle, and 7.3 ± 0.24 GBq (range, 6.95–7.60 GBq) for the fourth cycle. Whole-body scintigraphy was performed at least between 30–120 min, 24 h, and 6–8 d after administration of ^{177}Lu-PSMA I&T. In some cycles ($n = 8$), patients also underwent whole-body scintigraphy 48 and 72 h after the tracer injection. In detail, 26 cycles were analyzed with 3, 2 cycles with 4, and 6 cycles with 5 posttherapy scintigraphies, respectively. Details on the synthesis, application, and posttherapy scintigraphy of ^{177}Lu-PSMA I&T is given in the supplemental materials (supplemental materials are available at http://jnm.snmjournals.org).

Image Analysis

Individual patient absorbed doses for the whole body; kidneys; liver; and parotid, submandibular, and lacrimal glands were estimated based on the MIRD scheme and as recommended in the European Association of Nuclear Medicine Dosimetry Committee Guidelines (*18,19*). Regions of interest on the whole body; kidneys; liver; parotid, submandibular, and lacrimal glands; and up to 4 tumor lesions were delineated manually on the anterior and posterior whole-body images at 24 h after injection by 2 experienced nuclear medicine physicians and then manually relocated on the previous and subsequent scans (Fig. 1). The volumes of normal organs and tumor lesions were calculated using the CT dataset of the corresponding pretherapeutic ^{68}Ga-PSMA-HBED-CC PET/CT. A total of 93 representative lesions were analyzed (74 bone, 8 lymph node, 8 liver, 3 lung metastases; the assignment to the different cycles is shown in Table 2). Details on the regions of interest for scintigraphy and volume calculation in CT are given in the supplemental materials.

Statistical Analysis

All continuous data reported are expressed as mean, SD, and range. Two-sample *t* tests were used to evaluate differences between individual groups. Correlations between SUVs, change of SUV between pre- and posttherapeutic PET (ΔSUV), and absorbed dose in tumor lesions were assessed using Spearman rank correlation coefficient. A significance level of $\alpha = 5\%$ was used. Statistical analyses were conducted using MedCalc (version 13.2.0, 2014; MedCalc).

RESULTS

Qualitative ^{177}Lu-PSMA I&T Distribution on Posttherapeutic Scintigraphy

Physiologic uptake was seen in lacrimal, parotid, and submandibular glands; kidneys; small intestine; and less pronounced in the

TABLE 1
Effective Dose for Whole Body in Sv/GBq and Absorbed Doses for Normal Organs in Gy/GBq

Cycles investigated	Whole body	Kidneys*	Liver	Parotid glands*	Submandibular glands*	Lacrimal glands*
Overall ($n = 34$)						
Mean ± SD	0.06 ± 0.03†	0.72 ± 0.21	0.12 ± 0.06	0.55 ± 0.14	0.64 ± 0.40	3.8 ± 1.4
Range	0.02–0.11	0.33–1.22	0.05–0.26	0.25–0.84	0.24–1.70	1.68–7.03
First cycle ($n = 15$)						
Mean ± SD	0.05 ± 0.03	0.71 ± 0.25	0.12 ± 0.07	0.56 ± 0.17	0.54 ± 0.29	3.8 ± 1.5
Range	0.02–0.11	0.33–1.22	0.05–0.26	0.25–0.84	0.25–1.35	1.68–7.03
Second cycle ($n = 9$)						
Mean ± SD	0.06 ± 0.02	0.75 ± 0.19	0.13 ± 0.05	0.59 ± 0.13	0.71 ± 0.42	4.1 ± 1.1
Range	0.03–0.11	0.44–1.01	0.08–0.21	0.47–0.80	0.40–1.70	2.44–5.56
Third cycle ($n = 5$)						
Mean ± SD	0.06 ± 0.03	0.73 ± 0.22	0.12 ± 0.06	0.49 ± 0.11	0.83 ± 0.59	3.5 ± 1.4
Range	0.03–0.10	0.42–0.93	0.07–0.21	0.32–0.64	0.33–1.68	2.41–5.04
Fourth cycle ($n = 5$)						
Mean ± SD	0.05 ± 0.03	0.69 ± 0.18	0.11 ± 0.04	0.50 ± 0.11	0.66 ± 0.53	3.4 ± 1.7
Range	0.03–0.11	0.45–0.95	0.07–0.17	0.32–0.58	0.24–1.58	1.75–5.35

*Absorbed doses for paired organs are presented as average between right and left side.
†Median value: 0.03 Sv/GBq (for comparison with Baum et al.).

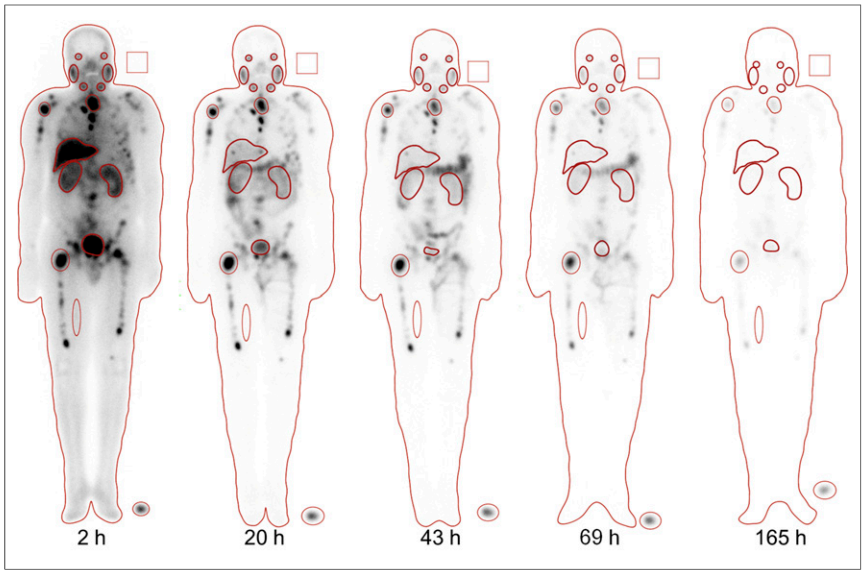

FIGURE 1. ^{177}Lu-PSMA I&T whole-body scintigraphy images obtained at 2, 20, 43, 69, and 165 h after administration. Regions of interest were drawn on liver, kidneys, parotid glands, submandibular glands, lacrimal glands, and lesions in right humerus, thoracic vertebrae, and right femur.

liver and spleen. Uptake in excess of background was also seen for multiple tumor lesions with progressive accumulation up to 24–48 h after injection (Fig. 1). Delayed whole-body images (up to 6–8 d after therapy) exhibited long-term retention of ^{177}Lu-PSMA I&T in the metastases, with nearly no residual uptake in normal organs.

Dosimetry for Normal Organs

The mean whole-body effective dose for all cycles was 0.41 ± 0.18 Sv (0.06 Sv/GBq). The mean absorbed organ doses were 5.3 ± 1.6 Gy (0.72 Gy/GBq) for the kidneys; 0.89 ± 0.42 Gy (0.12 Gy/GBq) for the liver; and 4.0 ± 1.1 Gy (0.55 Gy/GBq) for the parotid, 4.8 ± 2.8 Gy (0.64 Gy/GBq) for the submandibular, and 27 ± 10 Gy (3.8 Gy/GBq) for the lacrimal glands. The values (mean, SD, and ranges) for the corresponding absorbed doses per GBq are presented in Table 1. No substantial difference for absorbed doses of normal organs were observed when comparing them with respect to cycle number (Table 1; Fig. 2). The mean organ masses underlying these absorbed dose estimates were 1,595 ± 307 g (range, 1,165–2,373 g) for the liver, 153 ± 29.9 g (range, 88.4–218.7 g) for the kidneys, 19.1 ± 5.7 g (range, 8.0–35.6 g) for the parotid, 8.2 ± 1.9 g (range, 4.2–14.3 g) for the submandibular, and 0.45 ± 0.12 g (range, 0.25–0.78 g) for the lacrimal glands. For paired organs, masses from both sides were summed.

Dosimetry for Tumor Lesions

In total, all lesions received a mean dose per cycle of 23 ± 20 Gy (3.3 Gy/GBq). Mean absorbed dose for bone, lymph node, liver, and lung metastases were 26 ± 20 Gy (3.4 Gy/GBq), 24 ± 16 Gy (3.2 Gy/GBq), 8.5 ± 4.7 Gy (1.28 Gy/GBq), and 13 ± 7.4 Gy (1.7 Gy/GBq). The values (mean, SD, and range) for the corresponding absorbed doses per GBq are presented in Table 2. Figure 2 shows the mean absorbed dose in all tumor lesions with respect to the specific therapy cycle. Figure 3 shows a representative example of a patient with a histologically proven lung metastasis and multiple bone metastases. There is a clear trend toward a lower absorbed dose with an increasing number of the cycle. Mean absorbed dose per lesion was 26 ± 21 Gy (3.5 Gy/GBq) for the first, 24 ± 19 Gy (3.3 Gy/GBq) for the second, 20 ± 18 Gy (2.7 Gy/GBq) for the third, and 18 ± 17 Gy

TABLE 2
Absorbed Dose for Tumor Lesions in Gy/GBq

Cycles investigated	All metastases	Bone metastases	Lymph node metastases	Liver metastases	Lung metastasis
Overall (*n*)	93	74	8	8	3
Mean ± SD	3.2 ± 2.6	3.4 ± 2.7	3.2 ± 2.2	1.2 ± 0.67	1.75 ± 0.92
Range	0.22–12.03	0.22–12.03	1.63–8.46	0.47–2.59	0.94–2.68
First cycle (*n*)	41	33	5	2	1
Mean ± SD	3.5 ± 2.9	3.8 ± 3.1	2.6 ± 0.89	1.7	2.7
Range	0.22–12.03	0.22–12.03	1.63–3.76	0.85–2.59	
Second cycle (*n*)	26	21	2	2	1
Mean ± SD	3.3 ± 2.5	3.4 ± 2.4	5.2	0.94	1.3
Range	0.70–8.46	1.03–9.59	1.98–8.46	0.70–1.17	
Third cycle (*n*)	14	10	1	2	1
Mean ± SD	2.7 ± 2.3	3.2 ± 2.5	2.6	0.95	0.94
Range	0.94–7.99	1.11–7.99	18.87	0.47–1.42	
Fourth cycle (*n*)	12	10		2	
Mean ± SD	2.4 ± 2.2	2.7 ± 2.3		1.13	
Range	0.74–7.60	1.04–7.60		0.74–1.51	

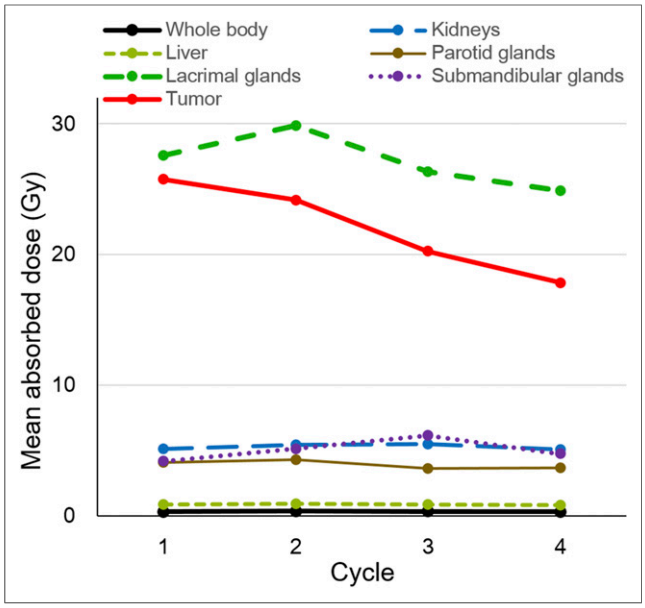

FIGURE 2. Absorbed doses for normal organs and tumors at respective cycle.

(2.4 Gy/GBq) for the fourth cycle. A similar trend can be seen for the subgroup of bone metastases. No reliable comparison is possible for lymph node, liver, and lung metastases because of a low sample number.

Correlation of SUV and Absorbed Doses in Tumor Lesions

The mean SUV_{max} and mean SUV_{mean} of all lesions in pretherapeutic PET were 22 ± 14 (range, 3.5–64.8) and 15 ± 10 (range, 2.4–46.8), respectively (Supplemental Table 2). The mean change in SUV (ΔSUV) was 4.8 ± 8.2 (range, −7.2–34.8) for SUV_{max} and 3.3 ± 5.7 (range, −4.8–24.1) for SUV_{mean}. SUV_{max} and SUV_{mean} moderately correlated with absorbed dose for all lesions ($r = 0.442$, $P < 0.001$ and $r = 0.433$, $P < 0.001$, respectively; Supplemental Table 2; Supplemental Fig. 1). Change of SUV_{max} and SUV_{mean} (ΔSUV) for all lesions showed a moderate and highly statistically significant correlation to the pretherapeutic SUV ($r = 0.468$, $P < 0.001$ for SUV_{max}; $r = 0.498$, $P < 0.001$ for SUV_{mean}; Supplemental Table 3). No correlation could be found between the change of SUV_{max} and SUV_{mean} (ΔSUV) for all lesions and the absorbed dose ($r = 0.163$, $P = 0.129$ for SUV_{max}; $r = 0.153$, $P = 0.154$ for SUV_{mean}; Supplemental Table 4). Details for both correlations on the subgroups of bone and soft-tissue lesions are shown in Supplemental Tables 2, 3, and 4.

DISCUSSION

We present data for radiation dosimetry for normal organs and tumor lesions using ^{177}Lu-PSMA I&T RLT in 18 patients and a total of 34 cycles. Our results for normal organs are comparable to recent clinical work on the safety and efficacy on ^{177}Lu-PSMA I&T including results on dosimetry (*7*) and data reported for ^{177}Lu-PSMA-DKFZ-617 (*9,11,12*). The kidneys are one of the critical organs, with a mean absorbed dose of 0.72 Gy/GBq and glandular tissue with high PSMA ligand uptake (lacrimal gland, 3.8 Gy/GBq; parotid gland, 0.55 Gy/GBq; and submandibular gland, 0.64 Gy/GBq). The long-term retention in tumor lesions resulted in a high mean absorbed tumor dose of 3.2 Gy/GBq, with a maximum of 12 Gy/GBq. In addition, high pretherapeutic SUV of a tumor lesion on PET may serve as rough indicator for a high absorbed dose, emphasizing the importance of pretherapeutic PSMA PET imaging for patient selection.

Data on the dosimetry are essential during the evaluation of new radiopharmaceuticals for radionuclide therapy to assess the risk of potential toxicity and response probability. There are common radiation tolerance limits as guiding values derived from external-beam radiation therapy. Thus, to some extent dose escalation studies can be omitted and dosing of new radiopharmaceuticals can be based on dosimetry. Qualitative judgment of the distribution of ^{177}Lu-PSMA I&T showed physiologic tracer uptake in the abdominal organs, especially the kidneys, as well as the lacrimal and salivary glands (*20*). Besides the high number of patients and total number of cycles included, a further strength of this study is the availability of a late (6–8 d after injection) time point for posttherapeutic scintigraphy. Baum et al. also included late scintigraphy for their ^{177}Lu-PSMA I&T dosimetry; however, only up to 5 d after injection (*7*). For ^{177}Lu-PSMA-DKFZ-617 it has been shown that (mainly) overestimation of doses is present when omitting the late time point (mean, 9.8% for whole body; 22.0% for kidney; 19.4% for salivary glands; 10.6% for lacrimal glands) (*12*).

In several radio-receptor therapies, the kidney is regarded as the dose-limiting organ (*21*). Our results for kidneys (mean, 0.72 Gy/GBq) are well comparable to a recent publication using the same radiopharmaceutical (kidney: median, 0.8 Gy/GBq) (*7*). For ^{177}Lu-PSMA-DKFZ-617, 3 recent reports state mean absorbed doses between 0.53 and 0.75 Gy/GBq for kidneys (*9,11,12*). These values are relatively comparable to that for the treatment of neuroendocrine tumors (for ^{177}Lu-DOTATATE, for example, 0.6 Gy/GBq (*22*)).

The whole-body absorbed dose determined in our study (mean, 0.06 Sv/GBq; median, 0.03 Sv/Gy) was slightly different from that found by Baum et al. (*7*) (median, 0.02 Gy/GBq), with only a higher maximum range. This is potentially based on a higher overall tumor burden in our patient cohort (median PSA, 354.5 ng/mL) as compared with Baum et al. (median PSA, 43.2 ng/mL). Because 15 of 18 patients in our study demonstrated extensive bone involvement, red marrow cross-doses might have been high. However, therapy-induced myelosupression was not noted on clinical follow-up.

Other organs at risk are salivary and lacrimal glands. For parotid and submandibular glands, the organ doses (mean, 0.55 and 0.64 Gy/GBq) derived from our study are lower than in the recent report for ^{177}Lu-PSMA I&T (median, 1.3 Gy/GBq) (*7*) and in the published data for ^{177}Lu-PSMA-DKFZ-617 (mean, 0.72–1.4 Gy/GBq) (*9,11,12*). The main reason is most likely variations of the volumes used for dose estimation. For salivary glands, for example, Hohberg et al. (*12*) used 85 g based on International Commission on Radiologic Protection 23 data whereas Delker et al. (*11*) used 38 g based on individual organ masses. Because of the high intraindividual size variation, we also aimed to use individual values based on CT images, with a mean volume for both sides of 54 g. In addition, further variation is possible due to different tracer distribution, different time points of posttherapy scintigraphy, and different overall tumor burden. Finally, the effect of cooling of salivary glands and posttherapeutic stimulation of saliva production is still unclear. Currently data are too sparse to estimate the potential benefit of the latter.

For the lacrimal glands, potential discrepancies are even more pronounced when performing dosimetry because of their small size on the lacrimal glands. So far, only Hohberg et al. evaluated the organ dose for lacrimal glands using ^{177}Lu-PSMA-DKFZ-617, with

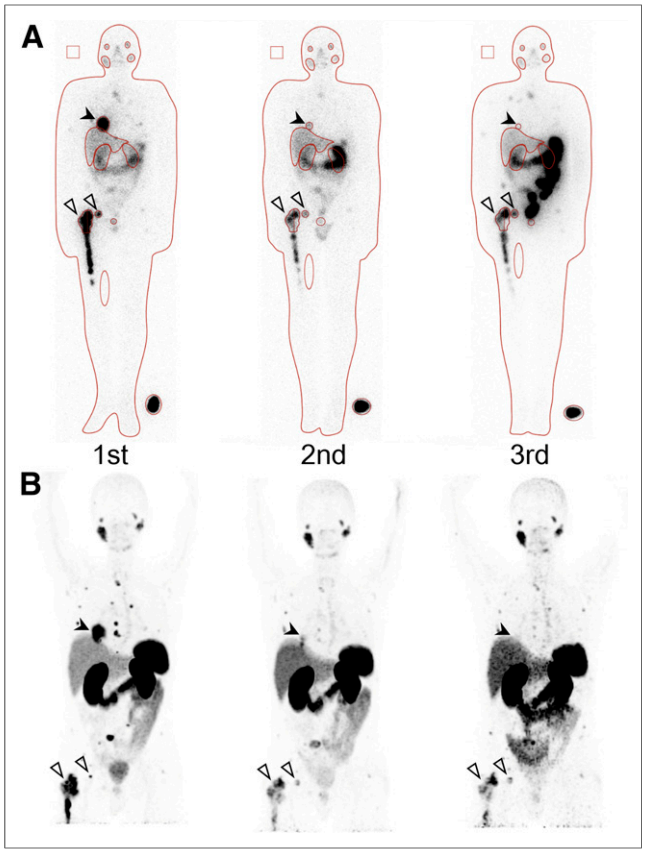

FIGURE 3. A 64-y-old patient with metastasis in lung (black arrow) and bone (white arrows). (A) Absorbed dose for lung metastasis for first, second, and third cycle were 20.9, 9.7, and 6.9 Gy, respectively. (B) SUV_{max} and SUV_{mean} on pretherapeutic PET at each cycle were 21.2, 9.9, and 3.7 and 13.8, 6.6, and 2.5, respectively.

a mean of 2.8 Gy/GBq. Our calculations resulted in a mean organ dose of 3.8 Gy/GBq. However, we most likely underestimated the size of the lacrimal glands (mean of 0.8 g) in CT compared with Hohberg et al. using a mass assumption of 1.4 g based on MR data (*12*). With a mean underestimation of volumes in our calculation (~42%), both results are quite comparable. However, despite the relatively high absorbed doses for salivary and lacrimal glands in clinical practice, they do not represent critical organs at risk. In our experience, despite the application of up to 30 GBq of ^{177}Lu-PSMA I&T, so far only sporadic cases of reversible xerostomia and no considerable complaints on dry eyes were noted (*10*). Hey et al., for example, using external-beam radiation therapy, reported that a dose to the parotid glands below 26 Gy allowed complete recovery of pretherapeutic salivary flow rates (*23*).

The absorbed doses (especially for the critical organs) showed an excellent correlation between the 4 therapy cycles. Delker et al. reported an overall Pearsons ρ of 0.97 when comparing the first and second cycle in 5 patients using ^{177}Lu-PSMA-DKFZ-617 (*11*). Similar results have been found for peptide receptor radionuclide therapy using up to 5 cycles (*24*). This might allow the prediction of the absorbed dose of the following therapy cycle with sufficient accuracy and the possibility of potential adaptation of the activity for the next cycle.

Our results for absorbed dose on tumor lesions (mean, 3.2 Gy/GBq) are comparable with data by Delker et al. (*11*) and Kratochwil et al. (*9*) for ^{177}Lu-PSMA-DKFZ-617 and with Baum et al. (*7*) for ^{177}Lu-PSMA I&T. In addition, we also analyzed and observed that the absorbed dose on the tumor was decreasing with the cycle number (Fig. 2; Table 2). In peptide receptor radionuclide therapy, this has also been reported for the use of ^{177}Lu-ocreotate (*25*). Compared with leukemia, most lymphomas and germ cell tumors and epithelial tumors such as neuroendocrine tumors and PC are only moderately radiosensitive and require a significantly higher dose of radiation. The reason for a decreasing absorbed dose remains unclear. Potential explanation could be prior therapy effect with reduced target expression (in later cycles predominantly patients were included with reasonable prior response). An indirect sign for this is the considerable drop of the PSA value in these patients, indicating therapy response with potential decreased presence of the target in the next cycle.

The highly significant and moderate correlation between pretherapeutic SUV and absorbed dose of ^{177}Lu-PSMA I&T (SUV_{max}: κ = 0.44, SUV_{mean}: κ = 0.43) stresses the importance of pretherapeutic PET imaging. Similar results are known for peptide receptor radionuclide therapy (*17*). Our initial data are a preliminary basis for estimating therapeutic efficacy (or feasibility) of PSMA RLT. The highly significant moderate correlation between pretherapeutic SUV and change of SUV (ΔSUV) fits into the concept that with a higher target expression a higher molecular response can be expected. Nevertheless, the missing correlation between absorbed dose and change of SUV (ΔSUV) indicates that besides target expression other factors of tumor biology are present for determination of therapy response. In addition, it has to be considered that more sophisticated approaches exist, which can be used to predict the therapeutic biodistribution. For example, Hardiansyah et al. recently presented a so-called physiologically based pharmacokinetic model that aims for individualization of treatment planned and integrates a variety of patient-specific data (e.g., weight, tumor volume, and glomerular filtration rate) (*26*).

With the kidneys being the relevant critical organ, our data indicate that on average a cumulative activity of 40 GBq of ^{177}Lu-PSMA I&T is safe when 28 Gy (50% probability of developing severe late kidney damage within 5 y) is the dose limit (*27*). With respect to the average life expectancy of mCRPC patients, this approach seems to be justifiable. This would allow at least 5 cycles using 7.4 GBq of ^{177}Lu-PSMA I&T (standard activity at our institution), achieving relevant absorbed doses on tumor lesions and offering the possibility of several cycles for midterm tumor control. These findings are in line with data presented by Kabaskal et al. using pretherapeutic dosimetry for ^{177}Lu-PSMA-DKFZ-617 and who calculated a maximum activity of 30 GBq to achieve a 23-Gy kidney dose (*13*). Nevertheless, these absorbed dose limits are based on the conventionally fractionated external-beam therapy and cannot necessarily be directly applied to low-dose-rate radiation (*28*). Patients without risk factors for kidney disease might tolerate a renal biologic equivalent dose up to 40 Gy, based on experience in NET (*29*).

There are several limitations of our study. First, the different peptides used for PET on one hand (PSMA-HBED-CC) and therapy on the other (PSMA I&T) are noteworthy. Second, one principal bias of dosimetry studies is the selection of tumor lesions that show better delineation from the surrounding healthy tissue and thus a relatively high absorbed dose. Numerous factors can impair the accuracy of PET and planar dosimetry and can lead to decreased correlation of the 2 modalities. Overlay in planar scintigraphy can lead to an overestimation of dose (*11,20*). SPECT should be the method of choice to avoid overlap with physiologic uptake and tumor uptake. Potential

additional errors can occur both for volumetric assessment and for measurement of SUV for the tumor lesions. We tried to minimize this error, by adjusting a volume of interest using information from PET to the anatomic configuration of the lesions. However, especially for bone lesions, the anatomic delineation can be difficult. On the other hand, SUV_{max} (as compared with SUV_{mean}) is a highly reproducible metric, with small expected error for quantification in the range of up to 10% (*30,31*). Third, we have not applied any sophisticated model in this study to aim for individual treatment planning. Fourth, it has to be stressed that the data comparing absorbed doses in different treatment cycles are not based on the same patients.

CONCLUSION

Organ- and tumor-absorbed doses for ^{177}Lu-PSMA I&T for RLT are comparable to recent reports using the same ligand as well as ^{177}Lu-PSMA-DKFZ-617. The kidneys represent the critical organ, with a mean absorbed dose of 0.72 Gy/GBq. Kidney-absorbed dose is relatively similar across different studies and is constant across several cycles in the same patient. When established dose limits from radiation oncology are used, up to 40 GBq of ^{177}Lu-PSMA I&T appear feasible, with limited risk of radiation-induced side-effects on normal organs given the average life expectancy for mCRPC patients. The preliminary correlation between pretherapeutic SUV and absorbed tumor dose emphasizes the need for initial PSMA ligand PET imaging for appropriate patient selection. Nevertheless, more data need to be collected from larger series to confirm and validate these initial findings.

DISCLOSURE

No potential conflict of interest relevant to this article was reported.

REFERENCES

1. Center MM, Jemal A, Lortet-Tieulent J, et al. International variation in prostate cancer incidence and mortality rates. *Eur Urol.* 2012;61:1079–1092.
2. Eiber M, Maurer T, Souvatzoglou M, et al. Evaluation of hybrid ^{68}Ga-PSMA ligand PET/CT in 248 patients with biochemical recurrence after radical prostatectomy. *J Nucl Med.* 2015;56:668–674.
3. Zechmann CM, Afshar-Oromieh A, Armor T, et al. Radiation dosimetry and first therapy results with a ^{124}I/^{131}I-labeled small molecule (MIP-1095) targeting PSMA for prostate cancer therapy. *Eur J Nucl Med Mol Imaging.* 2014;41:1280–1292.
4. Perner S, Hofer MD, Kim R, et al. Prostate-specific membrane antigen expression as a predictor of prostate cancer progression. *Hum Pathol.* 2007;38:696–701.
5. Lütje S, Heskamp S, Cornelissen AS, et al. PSMA ligands for radionuclide imaging and therapy of prostate cancer: clinical status. *Theranostics.* 2015;5:1388–1401.
6. Weineisen M, Simecek J, Schottelius M, Schwaiger M, Wester H-J. Synthesis and preclinical evaluation of DOTAGA-conjugated PSMA ligands for functional imaging and endoradiotherapy of prostate cancer. *EJNMMI Res.* 2014;4:63.
7. Baum RP, Kulkarni HR, Schuchardt C, et al. Lutetium-177 PSMA radioligand therapy of metastatic castration-resistant prostate cancer: safety and efficacy. *J Nucl Med.* January 21, 2016 [Epub ahead of print].
8. Ahmadzadehfar H, Eppard E, Kürpig S, et al. Therapeutic response and side effects of repeated radioligand therapy with ^{177}Lu-PSMA-DKFZ-617 of castrate-resistant metastatic prostate cancer. *Oncotarget.* 2016;7:12477–12488.
9. Kratochwil C, Giesel FL, Stefanova M, et al. PSMA-targeted radionuclide therapy of metastatic castration-resistant prostate cancer with Lu-177 labeled PSMA-617. *J Nucl Med.* 2016;57:1170–1176.
10. Heck MM, Retz M, D'Alessandria C, et al. Systemic radioligand therapy with ^{177}Lu-PSMA-I&T in patients with metastatic castration-resistant prostate cancer. *J Urol.* 2016;196:382–391.
11. Delker A, Fendler WP, Kratochwil C, et al. Dosimetry for ^{177}Lu-DKFZ-PSMA-617: a new radiopharmaceutical for the treatment of metastatic prostate cancer. *Eur J Nucl Med Mol Imaging.* 2016;43:42–51.
12. Hohberg M, Eschner W, Schmidt M, et al. Lacrimal glands may represent organs at risk for radionuclide therapy of prostate cancer with [^{177}Lu]DKFZ-PSMA-617. *Mol Imaging Biol.* 2016;18:437–445.
13. Kabasakal L, AbuQbeitah M, Aygün A, et al. Pre-therapeutic dosimetry of normal organs and tissues of ^{177}Lu-PSMA-617 prostate-specific membrane antigen (PSMA) inhibitor in patients with castration-resistant prostate cancer. *Eur J Nucl Med Mol Imaging.* 2015;42:1976–1983.
14. Waser B, Tamma M-L, Cescato R, Maecke HR, Reubi JC. Highly efficient in vivo agonist-induced internalization of sst2 receptors in somatostatin target tissues. *J Nucl Med.* 2009;50:936–941.
15. Cremonesi M, Botta F, Di Dia A, et al. Dosimetry for treatment with radiolabelled somatostatin analogues: a review. *Q J Nucl Med Mol Imaging.* 2010;54:37–51.
16. Kwekkeboom DJ, Teunissen JJ, Bakker WH, et al. Radiolabeled somatostatin analog [^{177}Lu-DOTA0,Tyr3]octreotate in patients with endocrine gastroenteropancreatic tumors. *J Clin Oncol.* 2005;23:2754–2762.
17. Ezziddin S, Lohmar J, Yong-Hing CJ, et al. Does the pretherapeutic tumor SUV in ^{68}Ga DOTATOC PET predict the absorbed dose of ^{177}Lu octreotate? *Clin Nucl Med.* 2012;37:e141–e147.
18. Hindorf C, Glatting G, Chiesa C, Lindén O, Flux G, EANM Dosimetry Committee. EANM Dosimetry Committee guidelines for bone marrow and whole-body dosimetry. *Eur J Nucl Med Mol Imaging.* 2010;37:1238–1250.
19. Siegel JA, Thomas SR, Stubbs JB, et al. MIRD pamphlet no. 16: techniques for quantitative radiopharmaceutical biodistribution data acquisition and analysis for use in human radiation dose estimates. *J Nucl Med.* 1999;40:37S–61S.
20. Afshar-Oromieh A, Malcher A, Eder M, et al. PET imaging with a [^{68}Ga]gallium-labelled PSMA ligand for the diagnosis of prostate cancer: biodistribution in humans and first evaluation of tumour lesions. *Eur J Nucl Med Mol Imaging.* 2013;40:486–495.
21. Bodei L, Cremonesi M, Grana CM, et al. Yttrium-labelled peptides for therapy of NET. *Eur J Nucl Med Mol Imaging.* 2012;39:S93–S102.
22. Sandström M, Garske-Román U, Granberg D, et al. Individualized dosimetry of kidney and bone marrow in patients undergoing ^{177}Lu-DOTA-octreotate treatment. *J Nucl Med.* 2013;54:33–41.
23. Hey J, Setz J, Gerlach R, et al. Parotid gland-recovery after radiotherapy in the head and neck region: 36 months follow-up of a prospective clinical study. *Radiat Oncol.* 2011;6:125.
24. Garske U, Sandström M, Johansson S, et al. Minor changes in effective half-life during fractionated ^{177}Lu-Octreotate therapy. *Acta Oncol.* 2012;51:86–96.
25. Garkavij M, Nickel M, Sjögreen-Gleisner K, et al. ^{177}Lu-[DOTA0,Tyr3] octreotate therapy in patients with disseminated neuroendocrine tumors: analysis of dosimetry with impact on future therapeutic strategy. *Cancer.* 2010;116(4, suppl):1084–1092.
26. Hardiansyah D, Maass C, Attarwala AA, et al. The role of patient-based treatment planning in peptide receptor radionuclide therapy. *Eur J Nucl Med Mol Imaging.* 2016;43:871–880.
27. Emami B, Lyman J, Brown A, et al. Three-dimensional photon treatment planning report of the collaborative working group on the evaluation of treatment planning for external photon beam radiotherapy tolerance of normal tissue to therapeutic irradiation. *Int J Radiat Oncol.* 1991;21:109–122.
28. Dale R, Carabe-Fernandez A. The radiobiology of conventional radiotherapy and its application to radionuclide therapy. *Cancer Biother Radiopharm.* 2005;20:47–51.
29. Bodei L, Cremonesi M, Ferrari M, et al. Long-term evaluation of renal toxicity after peptide receptor radionuclide therapy with ^{90}Y-DOTATOC and ^{177}Lu-DOTATATE: the role of associated risk factors. *Eur J Nucl Med Mol Imaging.* 2008;35:1847–1856.
30. Doot RK, Scheuermann JS, Christian PE, Karp JS, Kinahan PE. Instrumentation factors affecting variance and bias of quantifying tracer uptake with PET/CT. *Med Phys.* 2010;37:6035–6046.
31. Kinahan PE, Fletcher JW. PET/CT standardized uptake values (SUVs) in clinical practice and assessing response to therapy. *Semin Ultrasound CT MR.* 2010;31:496–505.